Magnetic Properties of Iron Ions in CoO(I) and CoO(II)†

HANG NAM OK* AND JAMES G. MULLEN
Purdue University, Lafayette, Indiana
(Received 8 November 1967)

Hyperfine Mössbauer spectra of Fe^{57} in cobaltous oxide in the pure and vacated forms are measured below the Néel temperatures. The hyperfine spectra of CoO(I) are of a pure Fe^{2+} type and give a pattern characteristic of magnetic and quadrupole hyperfine interactions. They are analyzed by diagonalizing a 4×4 magnetic and quadrupole interaction matrix of the first excited state of an Fe^{57} nucleus and fitting eight Lorentzians to the Mössbauer spectra. In connection with this analysis we have developed a general formalism which can give H, $\frac{1}{2}(e^2qQ)$, ϕ, θ, and η from Mössbauer data by using an IBM computer. Below 200°K, the magnetic hyperfine field at Fe^{57} nuclei in CoO(I) decreases with decreasing temperature, and has an internal field of magnitude 120 kG as its zero-point value. The quadrupole interaction increases with decreasing temperature, and the zero-point value of $\frac{1}{2}e^2qQ$ is -1.32 mm/sec for CoO(I). The tendency of the magnetic hyperfine field to decrease and the tendency of the quadrupole interaction to increase with decreasing temperature, as well as the temperature dependence of θ, ϕ, and η, can be explained by crystal-field theory in terms of temperature-dependent variations in the statistical population of electronic levels. The hyperfine Mössbauer spectra of CoO(II) below its Néel temperature consist of six lines, which are purely magnetic except for line broadening due to possible quadrupole interactions arising from defects which destroy long-range translational symmetry in this material. The zero-point value of the magnetic hyperfine field at Fe^{57} nuclei in CoO(II) is measured to be 553 kG. The temperature dependence of the magnetic hyperfine field for CoO(II) follows a Brillouin function for $S=\frac{3}{2}$ approximately, and its Néel temperature is measured to be 270 ± 10°K. The Mössbauer hyperfine spectra of the mixed form CoO(I, II) was also determined, and it is discussed in the framework of the model proposed in the previous paper. The magnetic hyperfine field and quadrupole coupling constant for the Fe^{2+} component of the Mössbauer spectra are found to be 150 kG and -1.01 mm/sec at 77°K, respectively, which are not in accord with the values previously reported by Wertheim.

I. INTRODUCTION

COBALTOUS oxide has been the subject of many recent x-ray, neutron-diffraction, and Mössbauer investigations.[1–7] Bizette[8] and La Blanchetais[9] reported that cobaltous oxide is an antiferromagnetic substance with a Néel temperature T_N of 291°K. According to Tombs and Rooksby's x-ray measurements,[10] the crystal structure of the cobaltous oxide is strictly of the NaCl type ($a_0=4.25$ Å at 20°C), whereas below T_N the lattice undergoes a slight contraction along the c axis, which increases gradually with decreasing temperature. Their results indicate that

$$c/a=0.995 \quad \text{at} \quad 203°\text{K}$$

and

$$c/a=0.988 \quad \text{at} \quad 93°\text{K}.$$

Saito, Nakahigashi, and Shimomura[6] show that

$$c/a=0.988 \quad \text{at} \quad 123°\text{K},$$

and they report a new rhombohedral deformation in addition to the well-known tetragonal deformation. From neutron-diffraction data, Roth[1] claimed that the spin direction for CoO is $[\bar{1}\bar{1}7]$, a direction which makes an angle of 11°31′ with respect to [001]. Using a high-resolution neutron diffractometer, van Laar[3,11] finds that his experimental results can be explained by either of the following two models: (a) a collinear rhombohedral spin arrangement with an angle between the c axis and the spin axis of 27.4°; (b) a multispin-axis tetragonal arrangement, consisting of four antiferromagnetic sublattices with different spin axes which also make an angle of 27.4° with respect to the c axis. He suggested that model (b) was preferable because CoO deforms tetragonally below its Néel temperature. The multispin-axis model was denied, however, by Nagamiya, Saito, Shimomura, and Uchida,[2] and also by Saito, Nakahigashi, and Shimomura,[6] who found a rhombohedral elongation, specified by the off-diagonal strain tensor components $e_{yz}=e_{zx}=e_{xy}$ of magnitude 5×10^{-4}. We have isolated two forms of cobaltous oxide and discussed many of their properties in our preceding paper. The form I, CoO(I), has a perfect NaCl structure and the form II, CoO(II), has an NaCl structure with half of the lattice sites vacant. The intermediate CoO(I, II), which was prepared and studied by most people in the past, is a mixture of CoO(I) and CoO(II) at 0°K, but it is not a simple mixture at higher temperatures because of the dispersion of anion vacancies from form II to form I. CoO(I) gives only Fe^{2+} lines in its Mössbauer spectrum, while CoO(II) gives only Fe^{3+} lines due to a large number of anion vacancies

* Based on a thesis research at Purdue University in partial fulfillment of the requirements for the degree of Doctor of Philosophy.

† Work supported in part by the U.S. Atomic Energy Commission, under Contract No. (AT11-1)1616.

[1] W. L. Roth, Phys. Rev. **110**, 1333 (1958).
[2] T. Nagamiya, S. Saito, Y. Shimomura, and E. Uchida, J. Phys. Soc. Japan **20**, 1285 (1965).
[3] B. van Laar, Phys. Rev. **138**, A584 (1965).
[4] G. K. Wertheim, Phys. Rev. **124**, 764 (1961).
[5] V. G. Bhide and G. K. Shenoy, Phys. Rev. **147**, 147 (1966).
[6] S. Saito, K. Nakahigashi, and Y. Shimomura, J. Phys. Soc. Japan **21**, 850 (1966).
[7] J. G. Mullen and H. N. Ok, Phys. Rev. Letters **17**, 287 (1966).
[8] H. Bizette, J. Phys. Radium **12**, 161 (1951).
[9] C. H. LaBlanchetais, J. Phys. Radium **12**, 765 (1951).
[10] N. C. Tombs and H. P. Rooksby, Nature **165**, 442 (1950).
[11] B. van Laar, J. Schweizer, and R. Lemaire, Phys. Rev. **141**, 538 (1966).

which may trap electrons. The intermediate CoO(I, II), of course, shows both Fe^{2+} and Fe^{3+} lines.

Mössbauer spectra of CoO(I) taken below the Néel point show a splitting due to the magnetic hyperfine interaction and quadrupole interaction at the Fe^{57} nucleus. The temperature dependence of the magnetic hyperfine field at Fe^{57} nuclei in CoO(I) has a maximum at about 180°K and then decreases monotonically with decreasing temperature, while the temperature dependence of the quadrupole interaction increases monotonically as the temperature decreases. A similar result was reported by Siegwarth[12] for divalent Fe^{57} in NiO. The tendency for the magnetic hyperfine field to decrease and the quadrupole interaction to increase with decreasing temperature at Fe^{57} nuclei in CoO(I) can be explained in terms of a statistical variation in the population of perturbed electronic levels under the spin-orbit coupling, the exchange interaction, and the effect of crystal distortion. Mössbauer spectra of CoO(II) taken below the Néel temperature show six-line magnetic hyperfine patterns characteristic of Fe^{3+}. The magnetic hyperfine field was found to follow a Brillouin function only to a rough approximation. Mössbauer spectra of CoO(I, II) consist of two sets of hyperfine patterns below the Néel temperature, one corresponding to Fe^{2+} and the other corresponding to Fe^{3+}. The hyperfine patterns of Fe^{2+} in CoO(I, II) are exactly the same as those of pure CoO(I), while those of Fe^{3+} in CoO(I, II) are almost the same as those of pure CoO(II) at low temperatures, but they have a higher Néel temperature than that of pure CoO(II).

II. THEORY

A. Hamiltonian for the Combined Magnetic Hyperfine and Electric Quadrupole Interaction

Recently, Mössbauer spectra have been used widely for investigations of the magnetic hyperfine field and quadrupole interaction at the site of a nucleus. The Hamiltonian for the $I=\frac{3}{2}$ first excited state of Fe^{57} may be written as[13]

$$\mathcal{H}_e=g_1\mu_N\mathbf{I}\cdot\mathbf{H}+[e^2qQ/2I(2I-1)][3I_{z'}{}^2-\mathbf{I}^2+\eta(I_{x'}{}^2-I_{y'}{}^2)],$$

where $x'y'z'$ represent the principal axes of the electric field gradient tensor, which are chosen so that $|V_{z'z'}|\geq|V_{y'y'}|\geq|V_{x'x'}|$, and where $\mathbf{H}$ is the internal magnetic field at the nucleus. The electric field gradient along z' is eq, and η is the asymmetry parameter in the $x'y'z'$ frame of reference. g_1 is the absolute value of the g factor for the first excited state of Fe^{57}, and μ_N is the nuclear magneton. Q is the nuclear quadrupole moment of the first excited state of Fe^{57} multiplied by the Sternheimer factor $(1-R)$. If $\mathbf{H}$ has a polar angle θ and an azimuthal angle of ϕ with respect to the $x'y'z'$ axes, and we take the quantization z axis along $\mathbf{H}$ and the x, y axes as shown in Fig. 1, $\mathcal{H}_e$ will become, on transforming from $x'y'z'$ to xyz,

$$\begin{aligned}\mathcal{H}_e=&I_z+\tfrac{1}{8}P(I_+I_-+I_-I_+)(3-\eta\cos2\phi)\sin^2\theta-\tfrac{1}{2}PI^2+\tfrac{1}{2}PI_z{}^2(3\cos^2\theta+\eta\sin^2\theta\cos2\phi)\\&+\tfrac{1}{4}P(I_+I_z+I_zI_+)[-3\sin\theta\cos\theta+\eta\sin\theta(\cos\theta\cos2\phi+i\sin2\phi)]+\tfrac{1}{8}PI_+{}^2[3\sin^2\theta+\eta\cos2\phi\\&\times(1+\cos^2\theta)+2i\eta\cos\theta\sin2\phi]+\tfrac{1}{4}P(I_-I_z+I_zI_-)[-3\sin\theta\cos\theta+\eta\sin\theta(\cos\theta\cos2\phi-i\sin2\phi)]\\&+\tfrac{1}{8}PI_-{}^2[3\sin^2\theta+\eta\cos2\phi(1+\cos^2\theta)-2i\eta\cos\theta\sin2\phi],\end{aligned}$$

where energies are expressed in units of $g_1\mu_NH$, and $P\equiv e^2qQ/6g_1\mu_NH$. In the above transformation the following relation between the primed and unprimed components of $\mathbf{I}$ is used:

$$\begin{pmatrix}I_x'\\I_y'\\I_z'\end{pmatrix}=\begin{pmatrix}\cos\theta\cos\phi & -\sin\phi & \sin\theta\cos\phi\\ \cos\theta\sin\phi & \cos\phi & \sin\theta\sin\phi\\ -\sin\theta & 0 & \cos\theta\end{pmatrix}\begin{pmatrix}I_x\\I_y\\I_z\end{pmatrix}.$$

The Hamiltonian matrix for the first excited state of Fe^{57} is

M_I \ M_I'	$\frac{3}{2}$	$\frac{1}{2}$	$-\frac{1}{2}$	$-\frac{3}{2}$
$\frac{3}{2}$	$\mathcal{H}_{11}$	$\mathcal{H}_{21}^*$	$\mathcal{H}_{31}^*$	0
$\frac{1}{2}$	$\mathcal{H}_{21}$	$\mathcal{H}_{22}$	0	$\mathcal{H}_{42}^*$
$-\frac{1}{2}$	$\mathcal{H}_{31}$	0	$\mathcal{H}_{33}$	$\mathcal{H}_{43}^*$
$-\frac{3}{2}$	0	$\mathcal{H}_{42}$	$\mathcal{H}_{43}$	$\mathcal{H}_{44}$

where asterisks stand for the complex conjugates, and

$$\begin{aligned}\mathcal{H}_{11}&=\tfrac{3}{2}+(9/8)P(3\cos^2\theta+\eta\sin^2\theta\cos2\phi)-(15/8)P+\tfrac{3}{8}P\\&\quad\times(3-\eta\cos2\phi)\sin^2\theta,\\\mathcal{H}_{22}&=\tfrac{1}{2}+\tfrac{7}{8}P(3-\eta\cos2\phi)\sin^2\theta\\&\quad+\tfrac{1}{8}P(3\cos^2\theta+\eta\sin^2\theta\cos2\phi)-(15/8)P,\\\mathcal{H}_{33}&=\mathcal{H}_{22}-1,\\\mathcal{H}_{44}&=\mathcal{H}_{11}-3,\\\mathcal{H}_{21}&=-\mathcal{H}_{43}=\tfrac{1}{2}\sqrt{3}P[-3\sin\theta\cos\theta\\&\quad+\eta\sin\theta(\cos\theta\cos2\phi-i\sin2\phi)],\\\mathcal{H}_{31}&=\mathcal{H}_{42}=\tfrac{1}{4}\sqrt{3}P[3\sin^2\theta+\eta\cos2\phi(1+\cos^2\theta)\\&\quad-2i\eta\cos\theta\sin2\phi].\end{aligned}$$

By diagonalizing the 4×4 matrix, one can obtain the energy eigenvalues T_n $(n=1, 2, 3, 4)$ of the first excited state of Fe^{57}, and the corresponding eigenvectors

$$|\phi_n\rangle=a_{1n}|\tfrac{3}{2},\tfrac{3}{2}\rangle+a_{2n}|\tfrac{3}{2},\tfrac{1}{2}\rangle+a_{3n}|\tfrac{3}{2},-\tfrac{1}{2}\rangle+a_{4n}|\tfrac{3}{2},-\tfrac{3}{2}\rangle.$$

[12] J. D. Siegwarth, Phys. Rev. **155**, 285 (1967).

[13] M. H. Cohen and F. Reif, *Solid State Physics*, edited by F. Seitz and D. Turnbull (Academic Press Inc., New York, 1957), Vol. 5.

On the other hand, since the ground state ($I=\frac{1}{2}$) has no quadrupole moment, the perturbed energies and their corresponding eigenvectors in the xyz frame will be

$$\tfrac{1}{2}(g_0\mu_N H) \mid \tfrac{1}{2}, -\tfrac{1}{2}\rangle$$

and

$$\tfrac{1}{2}(-g_0\mu_N H) \mid \tfrac{1}{2}, \tfrac{1}{2}\rangle,$$

where g_0 is the magnitude of the g factor of the ground state of Fe^{57} nuclei.

Since the γ-ray transitions between the first excited state and the ground state of Fe^{57} are of pure $M1$ type,[14] the transition probabilities between the four nondegenerate levels corresponding to the excited state and the two levels corresponding to the ground state (Fig. 2) can be calculated as follows: The transition probability of emitting a γ ray in the direction of $\mathbf{k}(\theta_k, \phi_k)$ for an $M1$-type transition of polarization M ($+1$ or -1) is proportional to[15]

$$T_{if}^{M}(\theta_k, \phi_k) = \Big| \sum_{M'=0,\pm1} \mathfrak{D}_{M'M}^{(1)*}(\theta_k, \phi_k, 0) \langle \psi_i \mid \sum_{i=1}^{A} (g_{s_i} s_i^{M'} + g_{l_i} l_i^{M'}) \mid \psi_f \rangle \Big|^2,$$

where (θ_k, ϕ_k) are the polar and azimuthal angles of $\mathbf{k}$ (the direction of γ-ray emission), $\mathfrak{D}^{(l)}(\theta_k, \phi_k, \chi_k)$ is the lth irreducible representation of the rotation group, and θ_k, ϕ_k, χ_k are the Euler angles of the coordinate transformation from the xyz system to a new system, which, in the present case, is such that the new z axis is along $\mathbf{k}$, and χ_k is taken to be zero for convenience. $\mathfrak{D}_{M'M}^{(1)}(\theta_k, \phi_k, 0)$ satisfy the orthogonality relation[16]

$$\int \mathfrak{D}_{M_1M_1'}^{(1)*}(\theta_k, \phi_k, 0)\mathfrak{D}_{M_2M_2'}^{(1)}(\theta_k, \phi_k, 0) \sin\theta_k d\theta_k d\phi_k = \tfrac{1}{3}(4\pi)\delta_{M_1M_2}\delta_{M_1'M_2'}.$$

For protons $g_{l_i}=1$, and for neutrons $g_{l_i}=0$, $g_{s_i}=$intrinsic g factor of the ith nucleon, $s_i^{M'}$, $l_i^{M'}=M'$ components of the spin and orbital angular momenta of ith nucleon ($M'=0, \pm1$), and ψ_i, $\psi_f=$initial and final nuclear wave functions. The intensity of the Mössbauer line, which corresponds to the transition $\mid \phi_n\rangle \rightarrow \mid \frac{1}{2}, m\rangle$ ($m=\frac{1}{2}$ or $-\frac{1}{2}$), is proportional to

$$\sum_{M=\pm1} \Big| \sum_{M'} \mathfrak{D}_{M'M}^{(1)*}(\theta_k, \phi_k, 0)\, a_{1n}{}^{*}\langle \tfrac{3}{2}, \tfrac{3}{2} \mid \mathfrak{N}_1{}^{M'} \mid \tfrac{1}{2}, m\rangle + \sum_{M'} \mathfrak{D}_{M'M}^{(1)*}(\theta_k, \phi_k, 0)\, a_{2n}{}^{*}\langle \tfrac{3}{2}, \tfrac{1}{2} \mid \mathfrak{N}_1{}^{M'} \mid \tfrac{1}{2}, m\rangle + \sum_{M'} \mathfrak{D}_{M'M}^{(1)*}(\theta_k, \phi_k, 0)\, a_{3n}{}^{*}\langle \tfrac{3}{2}, -\tfrac{1}{2} \mid \mathfrak{N}_1{}^{M'} \mid \tfrac{1}{2}, m\rangle + \sum_{M'} \mathfrak{D}_{M'M}^{(1)*}(\theta_k, \phi_k, 0)\, a_{4n}{}^{*}\langle \tfrac{3}{2}, -\tfrac{3}{2} \mid \mathfrak{N}_1{}^{M'} \mid \tfrac{1}{2}, m\rangle \Big|^2,$$

where $\mathfrak{N}_1{}^{M'} \equiv g_{s_i} s_i^{M'} + g_{l_i} l_i^{M'}$. For a polarization experiment, the summation over M should be dropped. By the Wigner-Eckart theorem each matrix element in the above expression is proportional to a Clebsch-Gordan coefficient. Therefore the relative intensities of the eight Mössbauer lines for a power sample having an isotropic Debye-Waller factor can be easily found by integrating the above expression over θ_k and ϕ_k, and using the orthogonality relation on $\mathfrak{D}_{M'M}^{(1)}(\theta_k, \phi_k, 0)$. If there is an angular dependence to the recoil-free fraction in the single-crystal case, then the intensity analysis given is not rigorously correct. Nevertheless, it should be approximately true in all cases except those involving exceptionally large anisotropies in the directional dependence of the binding. The results are shown in Table I, along with the corresponding energy of each allowed transition. It should be noted that the expressions for the relative intensities are much simpler than those reported elsewhere,[17,18] and in fact could have been written immediately by noting that the contributions of various a_{mn} components are always either 1, 2, or 3, depending on the change of magnetic quantum number relating to that component. By fitting the eight lines having the relative line positions and the relative intensities in Table I to Mössbauer data, one can find the optimum values of θ, ϕ, η, and P. The fifth parameter H is simply calculated from the proportionality constant of relative line positions (see column 2 in Table I). We can obtain $\frac{1}{2}(e^2qQ)$ from the relation

$$\tfrac{1}{2}(e^2qQ) = 3Pg_1\mu_N H.$$

Recently, Kündig[17] and Hoy and Chandra[18] treated the same problem discussed here, but they took the quantization axis along a principal axis of the electric field gradient. Their method requires the diagonalization of both 4×4 matrix for the excited state and a 2×2 matrix for the ground state, and gives a complicated expression for the relative intensities of the hyperfine lines. Our method, however, requires only the diagonalization of one 4×4 matrix which has four zero elements, and gives much simpler expressions for the Mössbauer line intensities (see Table I). For the most common cases ($\phi=0$ or $\pm90°$) our 4×4 matrix is real, which simplifies the calculation. Karyagin[19] has given a treatment of this problem from the same approach as used here, although his analysis is not so immediately applicable to computer techniques as the one given above.

[14] M. Goldhaber and A. W. Sunyar, Phys. Rev. **83**, 906 (1951).
[15] See, for example, M. A. Preston, *Physics of the Nucleus* (Addison-Wesley Publishing Co., Inc., Reading, Mass., 1962), Chap. 11.
[16] A. R. Edmonds, *Angular Momentum in Quantum Mechanics* (Princeton University Press, Princeton, N. J., 1957), Chap. 4.
[17] W. Kündig, Nucl. Instr. Methods **48**, 219 (1967).
[18] G. R. Hoy and S. Chandra, J. Chem. Phys. **47**, 961 (1967).
[19] S. V. Karyagin, Fiz. Tverd. Tela **8**, 493 (1966) [English transl.: Soviet Phys.—Solid State **8**, 391 (1966)].

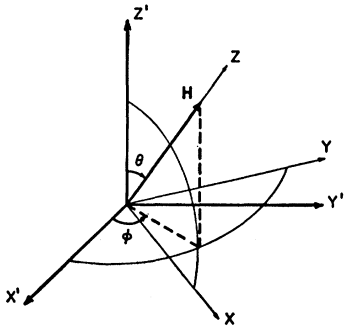

FIG. 1. Direction of **H** with respect to the principal axes x' y' z' of the electric field gradient tensor. In transforming from the $x'y'z'$ frame to the xyz frame, a rotation about z' of angle ϕ is followed by a rotation of angle θ about the y axis.

B. Crystal-Field Theory

The magnetic hyperfine field and the electric field gradient at a nucleus result from the surrounding electrons and ions. Consequently, in order to understand the origins and temperature dependences of the magnetic hyperfine field and the electric field gradient, it is necessary to know the splitting of the electronic levels caused by the crystal-field, spin-orbit coupling, and the exchange interaction. Since the interactions affecting electronic levels are different from material to material, we will restrict our argument to CoO(I). After obtaining the splittings for the electronic levels of Fe^{57} ions in CoO(I) by diagonalizing the perturbation matrix, we will calculate the contributions of each split level to the magnetic hyperfine field and the electric field gradient at the Fe^{57} nucleus. The ensemble averages of these contributions at each temperature will give the temperature dependences of the magnetic hyperfine field and electric field gradient. Finally, we shall try to explain the temperature dependences of the magnetic hyperfine field and electric field gradient obtained from our Mössbauer spectra (see Sec. A) in terms of the results obtained from crystal-field theory, using the method described above.

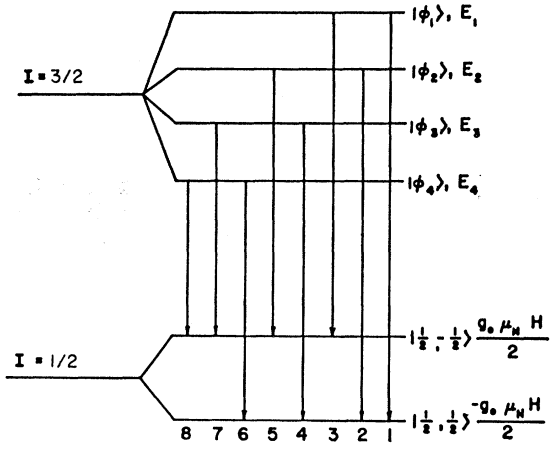

FIG. 2. Energy-level scheme for the first excited states and the ground states of an Fe^{57} nucleus.

According to Hund's rules, a free Fe^{2+} ion is in a ^5D state, which splits into d_γ and d_ϵ levels under the cubic octahedral field.[20,21] Since the d_γ levels are generally about 10^4 cm^{-1} higher than the d_ϵ levels, they do not contribute to the magnetic hyperfine field and electric field gradient at ordinary temperatures, and hence they will be neglected. The following three d_ϵ functions behave like the eigenfunctions of the angular momentum $l=1$ if we put $\mathbf{l}=-\mathbf{L}$, where $\mathbf{L}$ is proportional to the orbital angular momentum, and $\mathbf{l}$ can be considered as a pseudoangular momentum[20,22]:

$$\psi_1=Y_2^{-1},$$
$$\psi_0=(Y_2^{2}-Y_2^{-2})/\sqrt{2},$$
$$\psi_{-1}=-Y_2^{1}.$$

When the spin functions χ_j ($j=0, \pm1, \pm2$) are included, 15 wave functions ($\psi_i\chi_j$, $i=0, \pm1$, $j=0, \pm1, \pm2$) belong to the d_ϵ level. These 15-fold degenerate states will be split under the following perturbations[12,22]:

$$\mathcal{H}'=\lambda\mathbf{L}\cdot\mathbf{S}-2\sum_i J_i\mathbf{S}_i\cdot\mathbf{S}+\lambda\Delta(3l_z^2-2).$$

The first term represents the spin-orbit coupling. The spin-orbit coupling constant λ can be written[23] approximately as a product of the free-ion value λ_0 ($=-103$ cm^{-1} for a free Fe^{2+} ion) and a covalency factor α^2, which accounts for the decrease due to the covalency effect. The second term represents the Heisenberg exchange interaction between an Fe^{2+} spin $\mathbf{S}$ and host spin $\mathbf{S}_i$, and J_i is the exchange interaction constant between $\mathbf{S}_i$ and $\mathbf{S}$. The last term corresponds to the tetragonal distortion below the Néel temperature. Δ represents a proportionality constant and is assumed to be proportional to the fractional contraction of the lattice parameter c. As described in detail in the Intro-

TABLE I. The energies and relative intensities for Fe^{57} Mössbauer spectra under the combined magnetic hyperfine and electric quadrupole interaction.

Number	Energy	Relative intensity
1	$(g_1T_1+\frac{1}{2}g_0)\mu_NH$	$3\mid a_{11}\mid^2+2\mid a_{21}\mid^2+\mid a_{31}\mid^2$
2	$(g_1T_2+\frac{1}{2}g_0)\mu_NH$	$3\mid a_{12}\mid^2+2\mid a_{22}\mid^2+\mid a_{32}\mid^2$
3	$(g_1T_1-\frac{1}{2}g_0)\mu_NH$	$\mid a_{21}\mid^2+2\mid a_{31}\mid^2+3\mid a_{41}\mid^2$
4	$(g_1T_3+\frac{1}{2}g_0)\mu_NH$	$3\mid a_{13}\mid^2+2\mid a_{23}\mid^2+\mid a_{33}\mid^2$
5	$(g_1T_2-\frac{1}{2}g_0)\mu_NH$	$\mid a_{22}\mid^2+2\mid a_{32}\mid^2+3\mid a_{42}\mid^2$
6	$(g_1T_4+\frac{1}{2}g_0)\mu_NH$	$3\mid a_{14}\mid^2+2\mid a_{24}\mid^2+\mid a_{34}\mid^2$
7	$(g_1T_3-\frac{1}{2}g_0)\mu_NH$	$\mid a_{23}\mid^2+2\mid a_{33}\mid^2+3\mid a_{43}\mid^2$
8	$(g_1T_4-\frac{1}{2}g_0)\mu_NH$	$\mid a_{24}\mid^2+2\mid a_{34}\mid^2+3\mid a_{44}\mid^2$

[20] A. Abragram and M. H. L. Pryce, Proc. Roy. Soc. (London) **A205**, 135 (1951).
[21] B. Bleaney and K. W. H. Stevens, Rept. Progr. Phys. **16**, 130 (1953).
[22] J. Kanamori, Progr. Theoret. Phys. (Kyoto) **17**, 177 (1957).
[23] R. Ingalls, Phys. Rev. **133**, A787 (1964).

duction, many models on the spin arrangement in CoO have been suggested, but unfortunately, the detailed composition of most CoO samples used in earlier experiments were unknown. Since the usual methods of preparation of CoO give CoO(I, II), as shown in our preceding paper, samples were not likely to be pure CoO(I), which has a perfect NaCl structure with no vacancies. Therefore, we cannot accept without some reservation the results of the neutron-diffraction studies of the spin directions in CoO. We shall assume the collinear model, however, with the angle θ between the spin direction and [001] taken as an unknown for pure CoO(I). The spin direction of Co^{2+} with respect to the crystal axes is then $[\bar{1}, \bar{1}, \sqrt{2}\cot\theta_0]$. This collinear model is not vital to the analysis, but it is useful in relating θ_0 from the analysis to the spin orientation, because the spin will be parallel to the molecular field in this case.

In terms of the pseudoangular momentum **l**, assuming the validity of the molecular-field approximation,[22] we obtain for $\mathcal{H}'$

$$\mathcal{H}' = -\lambda \mathbf{l}\cdot\mathbf{S} + \lambda\beta\langle S_i\rangle \mathbf{M}\cdot\mathbf{S} + \lambda\Delta(3l_z^2 - 2),$$

where **M** is a unit vector in the molecular-field direction, β is the molecular-field constant, and $\langle S_i\rangle$ is the statistical average of $\mathbf{S}_i$. In order to obtain the energy levels and their corresponding eigenvectors, it is necessary to diagonalize the following 15×15 matrix:

$$\langle \psi_i\chi_j \mid \mathcal{H}' \mid \psi_{i'}\chi_{j'}\rangle,$$

where $i, i' = 0, \pm1$ and $j, j' = 0, \pm1, \pm2$. The solution of the secular equation will give the eigenvalues E_n, and the corresponding eigenfunctions can be expressed in the form

$$\Phi_n = \sum_{m=1}^{15} \Psi_m a_{mn},$$

where Ψ_m ($m = 1, 2, \cdots, 15$) is an abbreviation for the 15 wave functions, $\psi_i\chi_j$.

The effective magnetic field acting on a nucleus in a solid is regarded as the sum of the following contributions[24]:

(a) The field produced by the orbital magnetic moment on the parent atom,

$$\mathbf{H}_L = 2\mu_B\langle r^{-3}\rangle\langle \mathbf{L}\rangle\alpha^2,$$

where μ_B is the Bohr magneton and the expectation values refer to the 3*d* electron. The vector **r** refers to the vector distance from the nucleus to the 3*d* electron. **L** is the orbital angular momentum operator divided by $\hbar$.

(b) The field proportional to the spin density at the nucleus is

$$\mathbf{H}_S = (16\pi/3)\mu_B\langle \sum_i \mathbf{s}_i\delta(r_i)\rangle = \tfrac{1}{2}H_c\langle \mathbf{S}\rangle,$$

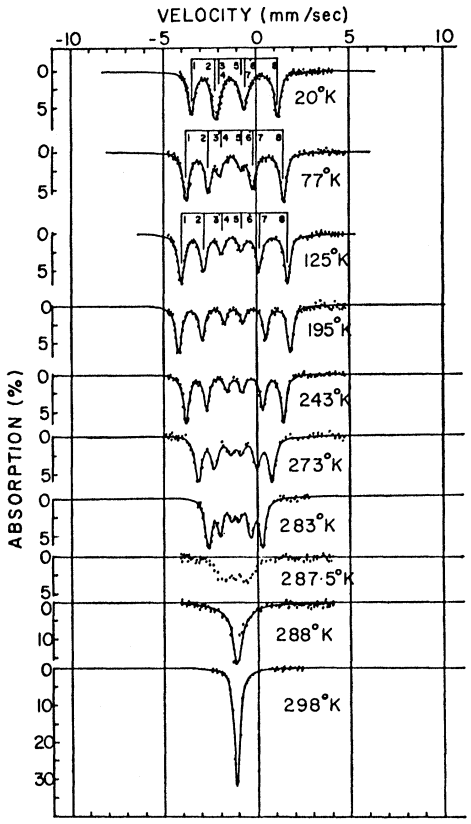

FIG. 3. Mössbauer spectra of CoO(I) below the Néel point at various temperatures. A 0.75-mg/cm² $Na_4Fe(CN)_6\cdot10\ H_2O$ absorber was used.

where H_c is the contact-term effective field and has been calculated to be about -550 kG for a free ion.[25] $\mathbf{s}_i$ is the spin angular momentum of the *i*th *s* electron divided by $\hbar$, and **S** is the net spin/$\hbar$ for the 3*d* shell. We assume here that the spin polarization of the *s* electrons is proportional to the spin of the 3*d* shell. The proportionality constant H_c is taken as a parameter in our analysis, and was generally found to be slightly smaller than the explicitly calculated free-ion value.

(c) The field produced by the dipolar interaction with the spin moment on the parent atom,

$$\mathbf{H}_D = 2\mu_B\langle 3\mathbf{r}(\mathbf{S}'\cdot\mathbf{r})r^{-5} - \mathbf{S}'r^{-3}\rangle$$
$$= -\tfrac{1}{2}\mu_B\langle 3\mathbf{r}(\mathbf{S}\cdot\mathbf{r})r^{-5} - \mathbf{S}r^{-3}\rangle,$$

where $\mathbf{S}'$ relates to the spin of the one 3*d* electron outside of the closed subshell with aligned spin, and **S** again relates to the net spin of all electrons in the 3*d* shell. If one takes

$$\mathbf{h}_D = [3\mathbf{S}\cdot(\mathbf{r}/r)]\mathbf{r}/r - \mathbf{S},$$

$\mathbf{H}_D$ can be written as

$$\mathbf{H}_D = -\tfrac{1}{2}\mu_B\langle r^{-3}\rangle\alpha^2\langle \mathbf{h}_D\rangle.$$

[24] W. Marshall and C. E. Johnson, J. Phys. Radium **23**, 733 (1962).

[25] R. E. Watson and A. J. Freeman, Phys. Rev. **123**, 2027 (1961).

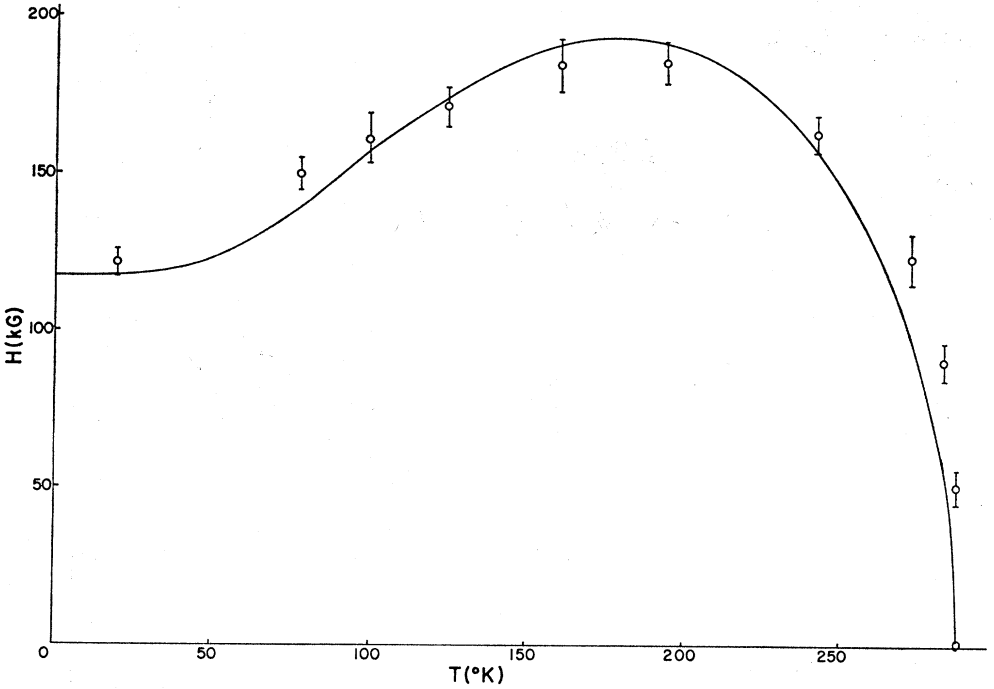

FIG. 4. Temperature dependence of the magnetic hyperfine field at Fe^{57} nuclei on CoO (I). The points with error bars are determined from Mössbauer spectra by diagonalizing the magnetic hyperfine and electric quadrupole interaction Hamiltonian matrix (4×4). The solid curve is determined by the crystal-field theory.

The total magnetic hyperfine field at the Fe^{57} nucleus is the sum of the above three contributions:

$$\mathbf{H}=\mathbf{H}_L+\mathbf{H}_S+\mathbf{H}_D.$$

Because the nuclear lifetime of the first excited state of Fe^{57} is only 10^{-7} sec, and the transitions between electronic states can be of order 10^{-8} sec or greater, it is not obvious that time averages and ensemble averages are equivalent, even though they are commonly assumed to be so.[12,23] We also shall assume that transition times between the 15 perturbed levels are sufficiently short as to permit ensemble averages of **L** and **S** for the case of CoO(I). For an operator O, the ensemble average can be written as

$$\langle O\rangle=\mathrm{Tr}O\rho,$$

where ρ is the density operator

$$\exp(-\mathcal{H}'/kT)/\mathrm{Tr}[\exp(-\mathcal{H}'/kT)].$$

Specifically, for a representation in which $\mathcal{H}'$ is diagonal,

TABLE II. Eigenenergies of $\mathcal{H}'$, their associated angular momenta, and quadrupole coupling constant below 100°K.

n	E_n (°K)	$\langle L_x\rangle_n$	$\langle L_z\rangle_n$	$\langle S_x\rangle_n$	$\langle S_z\rangle_n$	$\frac{1}{2}\langle e^2qQ\rangle_n$ (mm/sec)
15	720	0.351	0.868	−0.627	−1.792	−1.706
14	615	0.008	0.260	−0.492	−1.622	2.210
13	471	−0.097	−0.316	−0.391	−1.227	0.991
12	290	−0.170	−0.511	−0.179	−0.533	−0.513
11	275	0.215	0.679	−0.369	−1.113	0.670
10	210	−0.107	−0.345	−0.416	−1.244	−0.359
9	93	−0.235	−0.669	0.067	0.234	−0.492
8	−47	−0.020	−0.246	−0.059	−0.221	0.751
7	−103	0.179	0.680	−0.088	−0.244	−0.616
6	−112	−0.280	−0.788	0.316	1.024	−1.116
5	−304	−0.004	−0.180	0.277	0.742	1.799
4	−324	−0.318	−0.891	0.570	1.828	−1.715
3	−447	0.216	0.757	0.232	0.748	−0.950
2	−561	0.016	−0.141	0.606	1.676	2.870
1	−776	0.245	0.843	0.553	1.744	−1.348

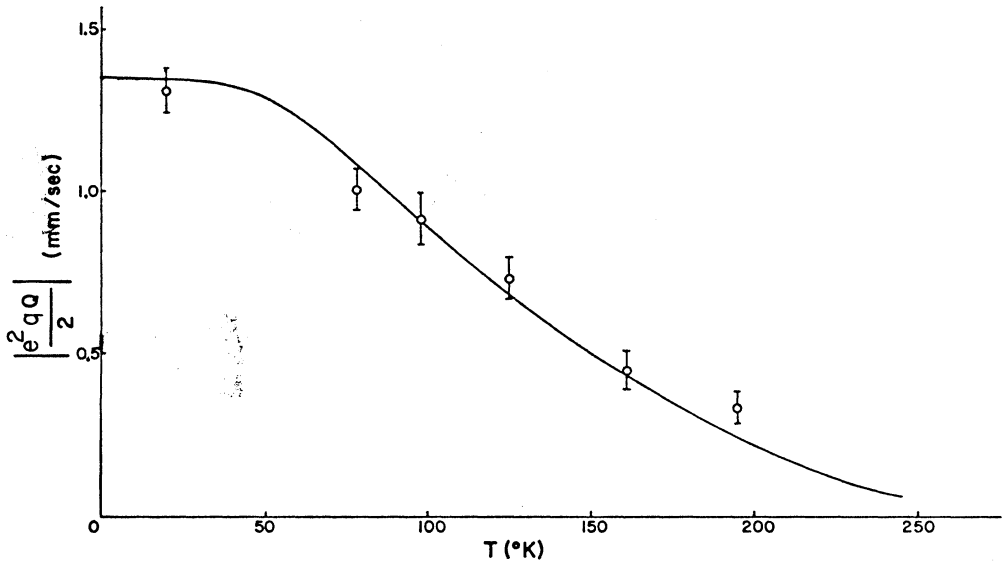

FIG. 5. Temperature dependence of $\frac{1}{2}(e^2qQ)$ in CoO(I).

$\langle O\rangle$ can be written explicitly as

$$\langle O\rangle = \sum_{n=1}^{15} O_{nn}\exp(-E_n/kT)/\sum_{n=1}^{15}\exp(-E_n/kT).$$

In this representation the following ensemble averages, $\langle\mathbf{L}\rangle$, $\langle\mathbf{S}\rangle$, and $\langle\mathbf{h}_D\rangle$, are easily calculated in accordance with the above prescription. The temperature dependence of the magnetic hyperfine field follows when the above $\langle\mathbf{L}\rangle$, $\langle\mathbf{S}\rangle$, and $\langle\mathbf{h}_D\rangle$ are substituted into the expressions for $\mathbf{H}_L$, $\mathbf{H}_S$, and $\mathbf{H}_D$. For the present case, including tetragonal distortion, $\mathbf{H}_L$, $\mathbf{H}_S$, and $\mathbf{H}_D$ are in general not parallel to $\mathbf{M}$.

The most important contribution to the electric field gradient at the Fe^{57} nucleus is due to the aspherical charge distribution of the $3d$ electrons belonging to the ferrous ion. The other smaller contribution arises from the charge distribution of the neighboring ions in the crystalline lattice, and it is neglected in this paper, because CoO(I) is almost cubic and the lattice contribution to the electric field gradient does not exceed 1% of that due to the $3d$ electron if one follows Ingalls' estimation.[23] The electric field gradient tensor due to the $3d$ electron outside of the half-filled $3d$ shell can be written as follows at a given temperature:

$$V_{ij} = -e\langle(3x_ix_j - r^2\delta_{ij})r^{-5}\rangle$$
$$= -e\langle r^{-3}\rangle\alpha^2\langle 3x_ix_jr^{-2} - \delta_{ij}\rangle,$$

where $x_1x_2x_3$ are the xyz coordinates of the $3d$ electron, and $i, j = 1, 2, 3$. In the last expression, $\langle 3x_ix_jr^{-2} - \delta_{ij}\rangle$ is the ensemble average of the expectation values of the bracketed terms. In order to get the principal axes of V_{ij}, it is necessary to diagonalize $\| V_{ij} \|$, i.e., $\mathbf{V}' = \mathbf{B}^{-1}\mathbf{V}\mathbf{B}$, where $\mathbf{B} = \| b_{ij} \|$, $\mathbf{V} = \| V_{ij} \|$, and $\mathbf{V}'$ is a diagonal matrix whose elements are arranged in such a way that

$$| V_{33}' | \geq | V_{22}' | \geq | V_{11}' |.$$

We take the coupling constant for the quadrupole interaction to be

$$\tfrac{1}{2}e^2qQ = \tfrac{1}{2}eQV_{33}',$$

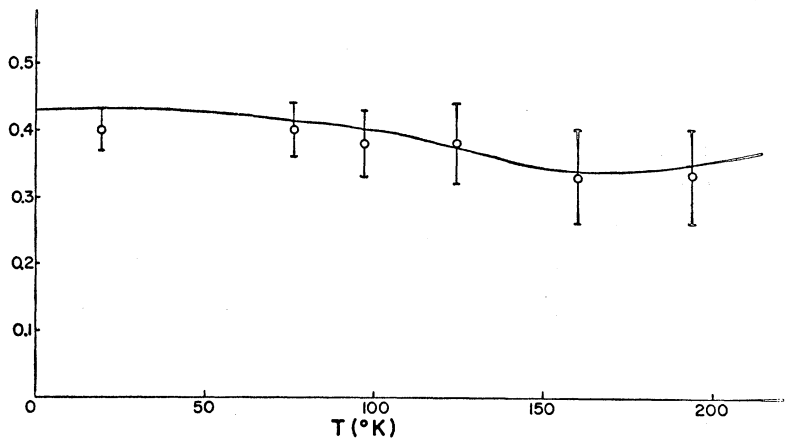

FIG. 6. Temperature dependence of η in CoO(I).

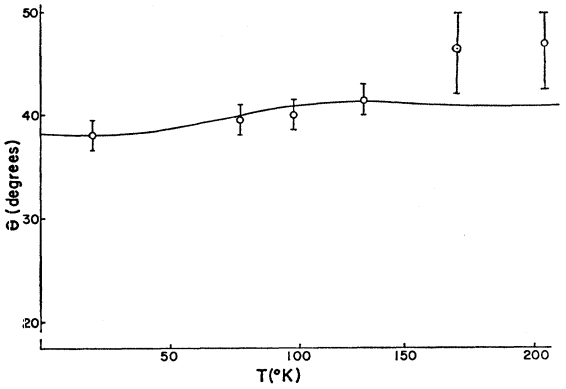

FIG. 7. Temperature dependence of θ in CoO(I).

where Q is the nuclear quadrupole moment of the first excited state of Fe^{57} multiplied by the Sternheimer factor $(1-R)$, which corrects for the polarization of the ferriclike (^6S, $3d^5$) core by the electric field gradient due to the $3d$ electron with opposed spin. The asymmetry factor η is given by

$$\eta=(V_{11}'-V_{22}')/V_{33}'.$$

The polar and azimuthal angles of **H** in the coordinate system of the principal axes of the electric field gradient tensor are

$$\theta=\cos^{-1}(H_xb_{13}+H_yb_{23}+H_zb_{33})/H$$

and

$$\phi=\tan^{-1}\frac{H_xb_{12}+H_yb_{22}+H_zb_{32}}{H_xb_{11}+H_yb_{21}+H_zb_{31}},$$

where H_x, H_y, and H_z are the cartesian components of **H**.

Using the above formalism, one can find the optimum values of H_c, α^2, $\langle r^{-3}\rangle$, Q, and the spin direction of the host Co^{2+}, such that the derived H, $\frac{1}{2}e^2qQ$, η, θ, and ϕ are fitted to those determined from experimental data described in Sec. IIA. $\beta\langle S_i\rangle$ and Δ are assumed to be proportional to the sublattice magnetization and lattice distortion, respectively, and the proportionality constants are also determined from the above fitting.

III. ANALYSIS OF EXPERIMENTAL DATA

A. CoO(I)

Mössbauer hyperfine spectra below the Néel temperature are shown in Fig. 3. The patterns indicate a pure magnetic hyperfine interaction from 288° to 243°K, but a contribution from the quadrupole interaction is evident for those resonances shown at $T=195$°K and below. Before trying to fit the eight lines in Table I to the data by varying θ, ϕ, η, and P, one may limit θ or ϕ to a few values by a simple symmetry argument. According to x-ray and neutron-diffraction experiments, the crystal distortion and spin arrangements are symmetrical about the (110) plane. Therefore, we may assume that one of the principal axes of the electric field gradient is perpendicular to the (110) plane, and that the other two principal axes and **H** are in the (110) plane. In this case only limited choices of ϕ or θ are possible; when the principal axis corresponding to the maximum field gradient is in the (110) plane, $\phi=\pm90°$ or 0°. When the z' axis is perpendicular to the (110) plane, $\theta=90°$. Using an IBM 7094 computer to fit the eight lines with the relative line positions and relative line intensities in Table I to the Mössbauer data of CoO(I) at each temperature, we find ϕ $(-90°)$, H, $\frac{1}{2}(e^2qQ)$, η, and θ as a function of temperature, as shown in Figs. 4 through 7. The data were fitted by assuming that the Mössbauer spectra consisted of eight Lorentzian curves, and the sum of the eight Lorentzians is drawn on the data points in Fig. 3, along with a schematic of the intensities of its constituent lines. In Fig. 4, the magnetic hyperfine field has a maximum at about 180°K, and then decreases with decreasing temperature. The same tendency was also observed in MnO and NiO by Siegwarth.[12] The quadrupole interaction, however, increases in magnitude with decreasing temperatures (Fig. 5). η and θ values are fairly constant under temperature variation, namely, about 0.40 ± 0.05 and about $42°\pm5°$, respectively (Figs. 6 and 7). From Fig. 3 the transition temperature from the hyperfine patterns to a single-line pattern is seen to be 288°K, which is 3° lower than the value measured by Bizette[8] and La Blanchetais.[9] This 3° discrepancy is outside of our experimental errors and probably reflects the limited accuracy of the earlier techniques.

We will try to explain temperature dependences of H, $\frac{1}{2}(e^2qQ)$, θ, and η in terms of the crystal-field theory developed in Sec. IIB. Using a Brillouin function with $S=\frac{3}{2}$ as an approximation of $\beta\langle S_i\rangle$ and varying the previously mentioned parameters, we tried to fit the theoretical H, $\frac{1}{2}(e^2qQ)$, θ, and η of the crystal-field theory to those obtained from the Mössbauer spectra, and found the following to be the optimum values:

$$\text{Spin direction}=[\bar{1}\bar{1}3],$$
$$H_c=-448\text{ kG},$$
$$\alpha^2=0.69,$$
$$\langle r^{-3}\rangle=4.4\text{ a.u.},$$
$$Q=0.21\text{ b}.$$

The zero-point values of $\beta\langle S_i\rangle$ and Δ were found to be 2.55 and 0.09, respectively. As expected, the calculation gave $-90°$ for ϕ at all temperatures. The theoretical curves are drawn in Figs. 4 through 7 (see solid lines) and are in good agreement with the values determined from Mössbauer spectra. The adjusted parameters are in reasonable agreement with currently reported values; $\langle r^{-3}\rangle=4.4$ a.u. is the same as Okiji and Kanamori's value[26]; $Q=0.21$ b, which contains the Sternheimer factor, is the same as Ingall's value.[23]

[26] A. Okiji and J. Kanamori, J. Phys. Soc. Japan **19**, 908 (1964).

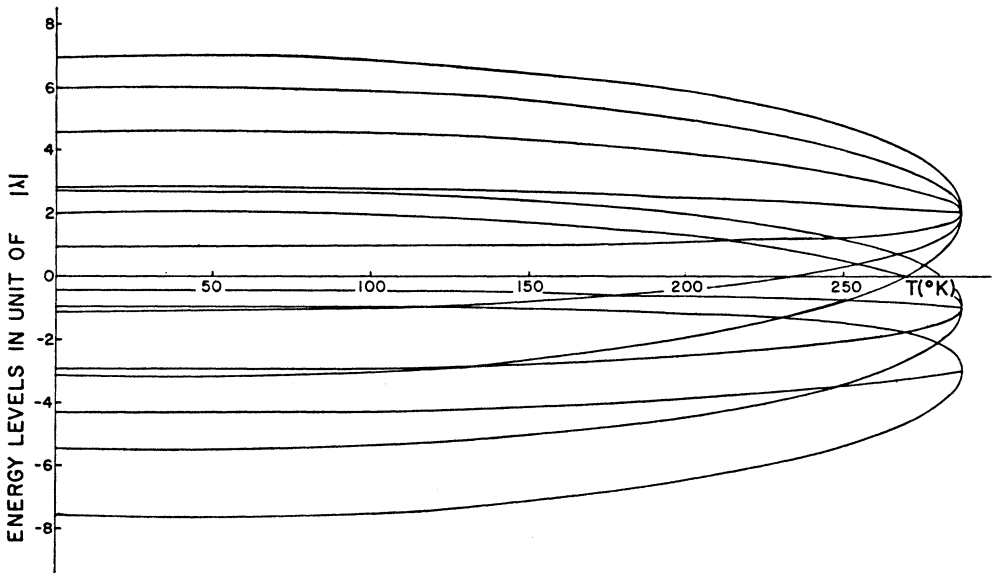

FIG. 8. Temperature dependence of the 15 energy levels of Fe^{2+} ion in CoO(I) originating from d_ϵ level. Energies are represented in units of the spin-orbit coupling constant ($|\lambda|=102.3°K$).

The spin direction $[\bar{1}\bar{1}3]$, which is 25° from the c axis, is almost the same as van Laar's value of $\theta_0=27.4°$. In Fig. 8, the temperature dependences of the 15 split energy levels are shown. Below about 100°K the energy levels and their eigenfunctions are almost independent of temperature, and therefore the temperature dependence of the magnetic hyperfine field can be easily understood from the statistical population of these levels. In Table II, the x and z components of $\langle\Phi_n|\mathbf{L}|\Phi_n\rangle$ and $\langle\Phi_n|\mathbf{S}|\Phi_n\rangle$ ($n=1, 2, \cdots, 15$) are shown along with their corresponding energy levels (the y components are the same as the x components by symmetry or by direct calculation). Orbital angular momentum in some lower excited states has the opposite sign to that in the ground state, while spin angular momentum in lower excited states has the same sign as that in the ground state (Table II). Therefore, the orbital angular momentum quenches more rapidly than the spin angular momentum with increasing temperature. The spin angular momentum $\langle\mathbf{S}\rangle$ and the orbital angular momentum $\langle\mathbf{L}\rangle$ give the opposite contributions to the magnetic hyperfine field (see the expressions for $\mathbf{H}_L$ and $\mathbf{H}_S$ in Sec. IIB). The ground-state contributions to the x, y, and z components are calculated to be

$$\langle\mathbf{H}_S\rangle_1=(-135, -135, -426)\ \text{kG},$$

$$\langle\mathbf{H}_L\rangle_1=(93, 93, 320)\ \text{kG},$$

$$\langle\mathbf{H}_D\rangle_1=(15, 15, -5)\ \text{kG}.$$

$\langle\mathbf{H}_S\rangle_1$ is largely cancelled by $\langle\mathbf{H}_L\rangle_1$ at very low temperatures, but since $\mathbf{H}_L$ decreases more rapidly in magnitude with increasing temperatures than $\mathbf{H}_S$, the cancellation decreases, thereby increasing the net magnitude of $\mathbf{H}$ with increasing temperatures. The ground-state wave function is

$$\Phi=0.088\psi_1\chi_0+0.092(-1+i)\psi_0\chi_2-0.312\psi_0\chi_1$$
$$-0.095(1+i)\psi_0\chi_0+0.873\psi_{-1}\chi_2+0.212(1+i)\psi_{-1}\chi_1,$$

where $\psi_i\chi_j$ components which are very small are neglected. The main contribution comes from the $\psi_{-1}\chi_2$ state. Since $\frac{1}{2}(e^2qQ)$ is -1.876 mm/sec for a ψ_{-1} state, the low-temperature value of -1.32 mm/sec obtained by direct analysis from Mössbauer spectra can be easily understood from the ground-state wave function. In

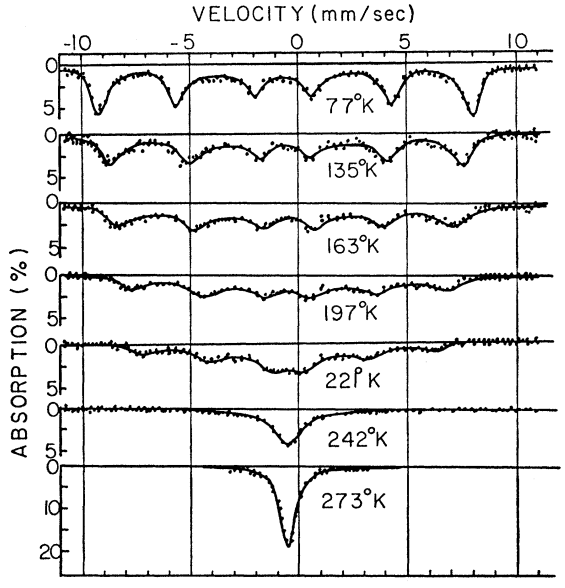

FIG. 9. Mössbauer hyperfine pattern of CoO(II) at various temperatures. A 1.0-mg/cm² $Na_4Fe(CN)_6\cdot 10H_2O$ absorber was used.

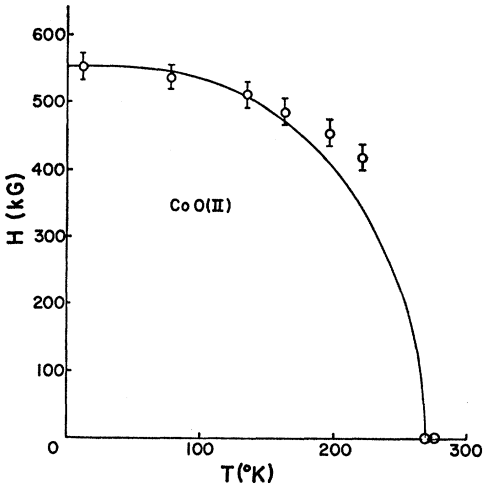

FIG. 10. Temperature dependence of the magnetic hyperfine field at Fe^{57} nuclei in CoO(II). The solid curve shows Brillouin function for $S=\frac{3}{2}$.

column 7 of Table II, $\frac{1}{2}(e^2qQ)$ for each of 15 split levels below 100°K is shown. Since the first excited state Φ_2 gives a large positive value of 2.870 mm/sec for $\frac{1}{2}(e^2qQ)$ in contrast to the negative ground-state value of -1.348 mm/sec, $\frac{1}{2}(e^2qQ)$ decreases very rapidly with increasing temperature (see Fig. 5).

It may be mentioned that Siegwarth[12] used an IBM computer subroutine which can only diagonalize real matrices, but since the actual Hamiltonian was a complex Hermitian matrix, he used a trick of rotating the whole crystal by a certain angle to get the eigenvectors and eigenvalues, thereby complicating the problem. We

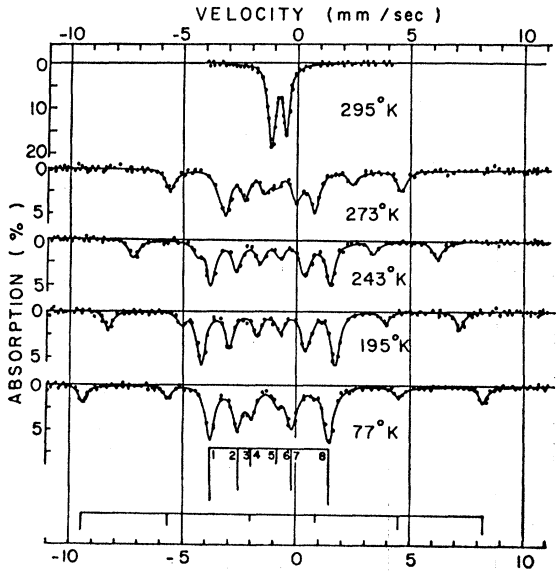

FIG. 11. Mössbauer spectra of CoO(I, II) below the Néel temperature. A 0.75-mg/cm² $Na_4Fe(CN)_6\cdot 10H_2O$ absorber was used.

used a computer program,[27] however, which can diagonalize any $N\times N$ Hermitian matrix ($N\leq 40$), and we diagonalized our Hermitian matrices without using this involved technique.

B. CoO(II)

Mössbauer spectra of CoO(II) at low temperatures are six-line patterns (Fig. 9), and almost purely magnetic. The hyperfine lines are broadened, however, which may be due to a quadrupole interaction with a random electric field gradient. The low-temperature values of the magnetic hyperfine field is 553 kG, which is typical of Fe^{3+}. The Fe^{3+} ions in CoO(II) are thought to originate from the trapping of electrons by anion vacancies discussed in detail in our preceding paper. The temperature dependence of the magnetic hyperfine field follows a Brillouin function for $S=\frac{3}{2}$ only approximately (Fig. 10). One noteworthy thing is that as the temperature increases, a broad unsplit line grows, in addition to the usual six-finger pattern, and becomes a relatively narrow single line as the temperature approaches the Néel point. This anomaly and the line broadening of the Mössbauer spectra were discussed in detail in our preceding paper. The Néel temperature was measured to be 270±10°K, which is slightly lower than the value of 288°K found for pure CoO(I).

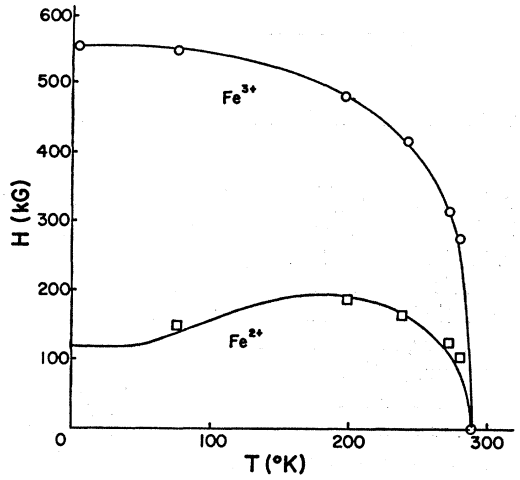

FIG. 12. Temperature dependence of the magnetic hyperfine field for Fe^{2+} and Fe^{3+} ions in CoO(I, II). The solid curve on the points of Fe^{2+} is the theoretical curve of CoO(I), and the solid curve on the points of Fe^{3+} is only a visual fit.

C. CoO(I, II)

As shown in our preceding paper, CoO(I, II) is a simple mixture of CoO(I) and CoO(II) at low temperatures. At elevated temperatures, however, anion vacancies appear to dissociate from form II and dis-

[27] This program is written by A. O'Hare and has the SDA number of 3368, which is available in Computer Science Center, Purdue University.

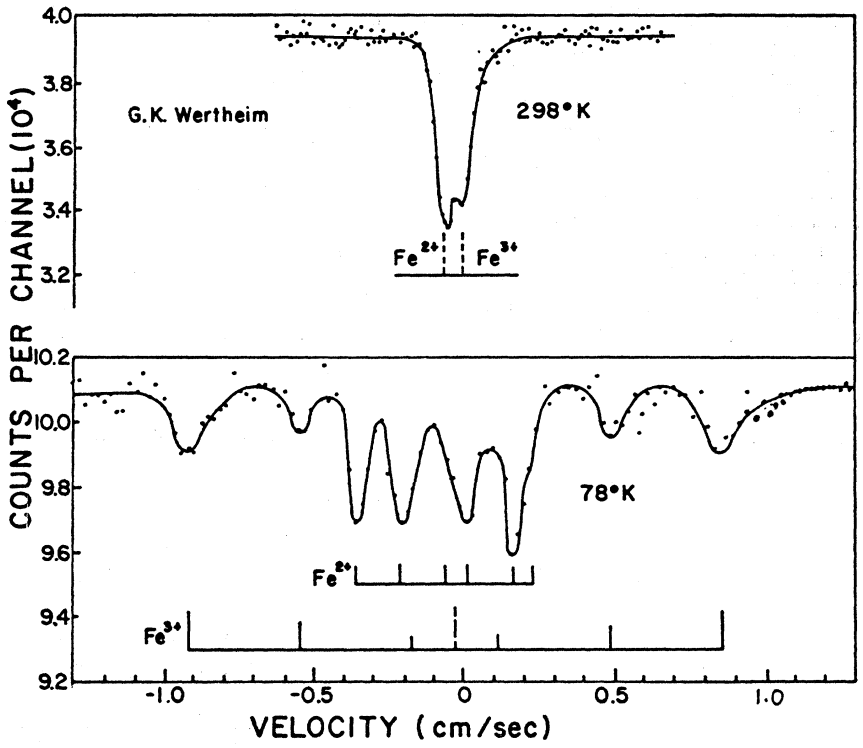

FIG. 13. Mössbauer spectra of CoO(I, II) at 78°K and room temperature reproduced from G. K. Wertheim [Phys. Rev. 124, 764 (1961)].

perse into form I in increasing numbers with increasing temperature. Therefore, the Mössbauer spectra of CoO(I, II) consist of Fe^{2+} lines and Fe^{3+} lines, as shown in Fig. 11. The temperature dependence of the magnetic hyperfine field and quadrupole interaction of Fe^{2+} in $CoO(I, II)_{C,T}$ ($C \leq 20\%$) is found to be the same as that of Fe^{57} in CoO(I) (compare Fig. 12 with Fig. 4). In particular, we found the following values of 77°K:

$$|H| = 150 \text{ kG}, \quad \tfrac{1}{2}(e^2qQ) = -1.01 \text{ mm/sec},$$
$$\theta = 39.5°, \quad P = -0.33.$$

Wertheim,[4] and later Bhide and Shenoy,[5] reported that a satisfactory fit was found at 78°K for

$$|H| = 180 \text{ kG}, \quad \tfrac{1}{2}(e^2qQ) = 31 \text{ Mc/sec} = 2.7 \text{ mm/sec},$$
$$\theta = 90°, \quad P = 0.35.$$

These results are not in agreement with our findings. For comparison, we list Wertheim's spectra at 78°K in Fig. 13. When one compares the spectra of Wertheim with our Figs. 3 and 11, it appears that he assigned only one line to the three lines (Nos. 2, 3, and 4) shown in Fig. 3. The magnetic hyperfine field of Fe^{3+} in $CoO(I, II)_{C,T}$ ($C \leq 20\%$) has nearly the same value at low temperatures as that of CoO(II), even though its Néel temperature is somewhat higher than that found for CoO(II), and in fact corresponds to that of CoO(I) (Fig. 12). An explanation of this observation is given in the previous paper.

IV. DISCUSSION

We have analyzed hyperfine Mössbauer spectra of CoO(I), CoO(II), and CoO(I, II), whose main properties were established in the preceding paper. In connection with this analysis we have developed a general formalism which can give H, $\frac{1}{2}(e^2qQ)$, θ, ϕ, and η from Mössbauer data by diagonalizing the interaction matrix related to the first excited state of Fe^{57} nuclei. Our formalism has simpler expressions for the intensity ratio for the eight lines than others reported in the literature,[17,18] and requires diagonalization of only one 4×4 matrix. Mössbauer spectra of CoO(I) consist of pure Fe^{2+} lines, and were fitted with eight lines at each temperature to give the temperature dependence of H, $\frac{1}{2}(e^2qQ)$, θ, η, and ϕ. ϕ is always $-90°$, and θ and η are approximately independent of temperature ($42°\pm5°$ and $0.40°\pm0.05°$, respectively). The quadrupole interaction increases with decreasing temperature, but unexpectedly, the magnetic hyperfine field decreases with decreasing temperature. The tendency for the magnetic hyperfine field to decrease and the quadrupole interaction to increase with decreasing temperature, as well as temperature dependences of θ, η, and ϕ, can be explained by crystal-field theory on the basis of temperature-dependent variations in the statistical population of the perturbed 15 levels originating from the d_ϵ level of Fe^{2+}. The values of H, $\frac{1}{2}(e^2qQ)$, η, θ, and ϕ determined from Mössbauer spectra by diagonalizing the 4×4 magnetic and quadrupole Hamiltonian matrix

are fitted very closely by those determined by crystal-field theory under the assumption of the spin-orbit coupling, Heisenberg exchange interaction, and tetragonal crystalline field (see Figs. 4 through 7). Points with error bars are determined by diagonalizing the 4×4 interaction matrix to fit Mössbauer spectra, and represent the estimated confidence in this fitting. The solid curves are determined from crystal-field theory. In this fitting, we adjusted various parameters, which turned out to be in reasonable agreement with those reported by others: $\langle r^{-3}\rangle=4.4$ a.u. and $Q=0.21$ b are essentially the same as those reported by others.[23,26] $H_c=-488$ kG is also nearly the same as -500 kG reported by Okiji and Kanamori.[26] The covalency factor α^2 for many ferrous compounds[23] is reported to be between 0.6 and 0.8, and our adjusted covalency factor of 0.69 is also in this region. This implies a spin-orbit coupling constant $\lambda=\alpha^2\lambda_0=102.3°$K. The spin direction of $[\bar{1}\bar{1}3]$ (that is, 25° from the c axis) is nearly the same as the 27.3° value reported by van Laar,[3] even though a comparison with these results is of limited value, because most samples of cobaltous oxides used by people in the past were probably CoO(I, II) instead of pure CoO(I).

PHYSICAL REVIEW VOLUME 168, NUMBER 2 10 APRIL 1968

Upper Bound on the Magnetoelectric Susceptibility

W. F. Brown, Jr.
Department of Electrical Engineering, University of Minnesota, Minneapolis, Minnesota
AND
R. M. Hornreich*† and S. Shtrikman*
Department of Electronics, The Weizmann Institute of Science, Rehovoth, Israel

The change in the free energy that occurs when electric and magnetic fields are simultaneously applied to a magnetoelectric medium is calculated. It is shown that a quadratic form related to this change in the free energy is positive definite, from which it follows that all elements of the magnetoelectric-susceptibility tensor must be smaller than the geometric mean of appropriate elements of the magnetic- and electric-susceptibility tensors. It is pointed out that the diamagnetic contribution to the magnetic-susceptibility tensor is negligible in materials in which the magnetoelectric effect is allowed. It is concluded that the magnetoelectric susceptibility should be small compared with unity, except possibly in ferroelectric or ferromagnetic materials.

INTRODUCTION

A MAGNETOELECTRIC medium is one in which there exists a linear relationship between an electric field and the medium's magnetic polarization and between a magnetic field and the medium's electric polarization. The possibility of such an effect was first pointed out by Landau and Lifshitz.[1] Subsequently, Dzyaloshinskii[2] predicted that the magnetoelectric effect should occur in Cr_2O_3. Experimentally, the effect was first seen by Astrov[3] in Cr_2O_3, and additional observations have been made on this and other materials by several investigators.[4–9]

The purpose of this paper is to show that the ordinary electric and magnetic susceptibilities provide an upper bound on the magnitude of the magnetoelectric effect. This is done by calculating the change in the free energy that occurs when electric and magnetic fields are simultaneously applied to a magnetoelectric medium. An expression for this energy change is obtained by using the method of "thermodynamic perturbation theory."[10] It is shown that a quadratic form related to this change in the free energy is positive definite, from which it follows that all elements of the magnetoelectric-susceptibility tensor must be smaller than the geometric mean of appropriate elements of the magnetic- and electric-susceptibility tensors.

* Research reported in this document sponsored in part by the Air Force Materials Laboratory Research and Technology Division AFSC through the European Office of Aerospace Research, U.S. Air Force Contract No. F61052-67-C-0040.

† Present address: Applied Research Laboratory, Sylvania Electronic Systems, Waltham, Mass.

[1] L. D. Landau and E. M. Lifshitz, *Electrodynamics of Continuous Media* (Addison-Wesley Publishing Co., Inc., Reading, Mass., 1960) (English transl. of a 1958 Russian edition), p. 119.

[2] I. E. Dzyaloshinskii, Zh. Eksperim. i Teor Fiz. **37**, 881 (1959) [English transl.: Soviet Phys.—JETP **10**, 628 (1960)].

[3] D. N. Astrov, Zh. Eksperim. i Teor. Fiz. **38**, 984 (1960); **40**, 1035 (1961) [English transls.: Soviet Phys.—JETP **11**, 708 (1960); **13**, 729 (1961)].

[4] V. J. Folen, G. T. Rado, and E. W. Stalder, Phys. Rev. Letters **6**, 607 (1961); G. T. Rado and V. J. Folen, *ibid.* **7**, 310 (1961).

[5] S. Shtrikman and D. Treves, Phys. Rev. **130**, 986 (1963).

[6] B. I. Al'shin and D. N. Astrov, Zh. Eksperim. i Teor. Fiz. **44**, 1195 (1963) [English transl.: Soviet Phys.—JETP **17**, 809 (1963)].

[7] G. T. Rado, Phys. Rev. Letters **13**, 335 (1964).

[8] E. Ascher, H. Rieder, H. Schmid, and H. Stossel, J. Appl. Phys. **37**, 1404 (1966).

[9] M. Mercier and J. Gareyte, Solid State Commun. **5**, 139 (1967).

[10] L. D. Landau and E. M. Lifshitz, *Statistical Physics* (Addison-Wesley Publishing Co., Inc., Reading, Mass., 1958) (English transl. of a 1953 Russian edition), p. 93; see also Ref. 1, pp. 63 and 131.